Journal of Molecular Structure 1027 (2012) 70–80

Contents lists available at SciVerse ScienceDirect

Journal of Molecular Structure

journal homepage: www.elsevier.com/locate/molstruc

Benzotristhiazole based chromophores for nonlinear optics

Andrea Fülöpová [a], Peter Magdolen [a,*], Ivica Sigmundová [a], Pavol Zahradník [a], Erik Rakovský [b], Marek Cigáň [c]

[a] Department of Organic Chemistry, Faculty of Natural Sciences, Comenius University, Mlynská dolina, 842 15 Bratislava, Slovak Republic
[b] Department of Inorganic Chemistry, Faculty of Natural Sciences, Comenius University, Mlynská dolina, 842 15 Bratislava, Slovak Republic
[c] Chemical Institute, Faculty of Natural Sciences, Comenius University, Mlynská dolina, 842 15 Bratislava, Slovak Republic

HIGHLIGHTS

- ▶ Various methylations of unsymmetrical trimethylbenzotristhiazole were studied.
- ▶ The structure of the obtained monomethylated salt was proved by X-ray analysis.
- ▶ The X-ray analysis was in accord with the quantum-chemical calculations (DFT-B3LYP).
- ▶ A series of condensation products with push–pull structure was prepared.
- ▶ Relations between structure, linear and nonlinear optical properties were examined.

ARTICLE INFO

Article history:
Received 24 April 2012
Received in revised form 8 June 2012
Accepted 11 June 2012
Available online xxxx

Keywords:
Benzotristhiazole
Azolium salts
X-ray analysis
DFT calculations
Hyperpolarizability
UV–Vis spectra

ABSTRACT

Methylation of unsymmetrical trimethylbenzotristhiazole with various reagents has been studied in details. The structure of obtained 2,3,5,8-tetramethylbisthiazolo[4,5-e;5,4-g]-1,3-benzothiazolium iodide has been proved by X-ray analysis in accord with the quantum-chemical calculations at DFT-B3LYP level. The electron-withdrawing tetramethylbenzotristhiazolium building block was submitted to Knoevenagel reaction with aromatic aldehydes containing an electron-releasing group. This led to a series of condensation products with push–pull structure. Relations between structure, linear (UV–Vis and fluorescence spectra) and nonlinear optical properties (calculated frontier orbital energy gap, BLA index, hyperpolarizabilities β and γ) have been investigated.

1. Introduction

Organic molecules exhibiting sufficient nonlinear optical (NLO) response (first or second hyperpolarizabilities – β, γ; two-photon absorption – TPA) have obtained a great deal of attention for their potential application as active elements in optoelectronic devices including microscopy [1,2], optical power limiting [3], photodynamic therapy [4], up-converted lasing [5], optical data storage [6], and microfabrication [7]. The quantitative measures of NLO-response are expressed by the experimental or theoretical values of hyperpolarizabilities β or γ, while the efficiency of two-photon absorption is quantified by the calculated or measured TPA cross-sections σ_{TPA}.

It was shown that chromophores containing a π-deficient heterocyclic ring (pyridine, quinoline, benzothiazole) as well as a π-excessive unit (thiophene, pyrrole, carbazole) were found as highly efficient NLO-phores [8–11]. The heterocyclic ring also brings photochemical and thermal stability into the molecule.

In addition to the classical push–pull dipolar molecules where a linear charge transfer is the principal factor of optical nonlinearity, compounds with quadrupolar, octupolar, multiple-branched, or dendrimeric structures have been reported displaying important cooperative effects leading to enhanced NLO-response [12,13].

Recently, we have published a six-step synthesis of the unsymmetrical benzotristhiazole (BTT) unit (Scheme 4) as a novel electron-withdrawing core for construction of possible NLO chromophores [14].

Continuing our work in this line, we herein wish to report the synthesis and study of compounds based on benzotristhiazole building block. To increase the electron-withdrawing strength of the heterocyclic central core, we have tried to quaternize the thiazole nitrogen. In addition to the improvements of the electronic structure of the molecule, the ionic compounds are especially

---

* Corresponding author. Tel.: +421 2 60296603; fax: +421 2 60296337.
E-mail address: magdolen@fns.uniba.sk (P. Magdolen).

0022-2860/$ - see front matter © 2012 Published by Elsevier B.V.
http://dx.doi.org/10.1016/j.molstruc.2012.06.018

attractive among the wide range of NLO-phores due to their high stability and tailorability.

The asymmetry of the starting benzotristhiazole induces small differences in the nucleophilicity of the heterocyclic nitrogen atoms. These variations were also predicted by the quantum chemical calculations. Methylation of the starting benzotristhiazole produced a mixture of two monomethylated isomers; in some cases also dimethylated products were formed. The yield and the ratio of the *N*-methylated products were influenced by the alkylating agent and reaction conditions. The right structure of the prevailing monomethylated product has been determined by X-ray analysis.

The one-armed condensation products of the *N*-methyl salt have been prepared by the Knoevenagel reaction with aromatic aldehydes containing an electron-releasing group.

2. Experimental part

2.1. General remarks

1,2-Dichloroethane was dried using a common method – reflux on CaH_2. For reactions performed under microwave irradiation either the reactor Anton Paar Monowave 300 (max. power 850 W) or the reactor Initiator™ BIOTAGE (max. power 300 W) were used. Melting points were measured on a Kofler apparatus Electrothermal IA-9200 and were not corrected. ^{1}H NMR and ^{13}C NMR spectra were recorded either on a Varian NMR System™ 300 (300 MHz) spectrometer, or in some cases a Varian NMR System™ 600 (600 MHz) was used. ^{15}N chemical shifts were measured indirectly, via $^{1}H—^{15}N$ long range correlation on a Varian NMR System™ 600 MHz spectrometer. The chemical shifts were referenced to a tetramethylsilane standard, the shifts for ^{15}N spectra are given on the nitromethane scale. IR spectra were recorded on Thermo Scientific Nicolet iS10 spectrometer (Smart iTR diamond ATR). Electronic absorption spectra were obtained on a Jenway 6705 UV/Vis spectrophotometer and fluorescence measurements were performed on an Edinburgh Instruments FSP 920 spectrofluorimeter. The fluorescent quantum yield of derivatives **3a**–**3f** in solution was determined using Rhodamine 101 in EtOH as the standard, taking the quantum yield of Rhodamine 101 in EtOH equal to 1.00 [15]. In the condensation reactions several aldehydes were used, which are either commercially available (4-(dimethylamino)benzaldehyde and 4-(dimethylamino)cinnamaldehyde) or were prepared according to the literature: (2*E*,4*E*)-5-[4-(*N*,*N*-dimethylamino)phenyl]penta-2,4-dienal [16], 4-(diphenylamino)benzaldehyde [17], (2*E*)-3-[4-(*N*,*N*-diphenylamino)phenyl]propenal [18], julolidine-9-carbaldehyde [19].

2.2. Synthesis

2.2.1. 2,3,5,8-tetramethylbisthiazolo[4,5-e; 5,4-g]-1,3-benzothiazolium iodide (2b)

In a glass vessel for microwave reactor the compound **1** (0.3 g, 0.001 mol) was partly dissolved in methanol (20 mL). Methyl iodide (3.1 mL, 0.05 mol, 50 eq.) was added and the reaction mixture was exposed to microwave irradiation for 2 × 20 min at 115 °C. The brownish precipitate (mixture of **2a** and **2b** in a ratio of 15:85) was filtered off. The crude product (0.250 g) was crystallized twice from methanol to get green crystals of **2b**.

Yield: 0.067 g (15%); mp 230–233 °C. *Anal.*: Calcd for $C_{13}H_{12}IN_3S_3\cdots 1/2\,CH_3OH$: C, 36.08; H, 3.14; N, 9.35; S, 21.41. Found: C, 35.64; H, 2.98; N, 9.04; S, 21.39. IR (powder film): ν = 3510 and 3435 (—OH in CH_3OH, H-bonded), 3047, 2974 and 2929 and 2900 and 2859 (C_{sp3}—H), 2721, 2379, 1983, 1603 and 1578 (C_{Ar}=C_{Ar}), 1506, 1429, 1365, 1163 cm^{-1}. ^{1}H NMR ($(CD_3)_2SO$, 300 MHz): δ = 4.80 (s, 3H, N^{+}—CH_3), 3.29 (s, 3H, CH_3), 3.16 (d, *J* = 4.3 Hz, CH_3 from CH_3OH), 3.05 (s, 3H, CH_3), 3.010 (s, 3H, CH_3). ^{13}C NMR ($(CD_3)_2SO$, 75 MHz): δ = 175.2, 171.7, 169.1, 142.1, 138.3, 133.4, 129.9, 126.7, 121.1, 48.5 (CH_3 from CH_3OH), 39.5, 20.1, 19.9, 17.24. ^{15}N NMR ($(CD_3)_2SO$, 600 MHz): δ = −79.7, −83.3, −184.1.

2.2.2. General procedure for preparation of 3a–3f

In a glass vessel for microwave reactor the compound **2b** (0.1 g, 0.23 mmol) was partly dissolved in methanol (10 mL). The appropriate aldehyde (0.242 mmol, 1.05 eq.) was added and the reaction mixture was exposed to microwave irradiation. For accurate temperatures, reaction times and obtained pressures see bellow in Table 1. When the reaction was finished the dark precipitate with metallic lustre was filtered off and washed with diethyl ether.

2.2.3. 2-{(E)-2-[4-(dimethylamino)-phenyl]vinyl}-3,5,8-trimethylbisthiazolo[4,5-e; 5,4-g]-1,3-benzothiazolium iodide (3a)

mp 317–320 °C (the dark color changes to orange at 270 °C). *Anal.*: Calcd. for $C_{22}H_{21}IN_4S_3$: C, 46.81; H, 3.75; N, 9.92; S, 17.04. Found: C, 46.72; H, 3.47; N, 9.66; S, 17.09. IR (powder film): ν = 3041 and 3009 (=C—H, C_{Ar}—H), 2962 and 2906 and 2856 and 2820 (C_{sp3}—H), 2686, 1729, 1611 and 1573 (C=C, C_{Ar}=C_{Ar}), 1520, 1432, 1366, 1259, 1092, 1020, 793 cm^{-1}. ^{1}H NMR ($(CD_3)_2SO$, 600 MHz): δ = 8.18 (d, *J* = 15.2 Hz, 1H, CH=), 7.86 (d, *J* = 8.8 Hz, 2H, C_{Ar}—H), 7.63 (d, *J* = 15.2 Hz, 1H, CH=), 6.78 (d, *J* = 9.2 Hz, 2H, C_{Ar}—H), 4.81 (s, 3H, N^{+}—CH_3), 3.10 (s, 6H, N—$(CH_3)_2$), 3.03 (s, 3H, CH_3), 2.99 (s, 3H, CH_3). ^{13}C NMR ($(CD_3)_2SO$, 150.8 MHz): δ = 171.2, 169.9, 168.3, 153.4, 150.2, 142.2, 138.0, 133.3, 132.8 (2 × C), 129.3, 125.7, 121.4, 118.5, 111.8 (2 × C), 105.6, 39.6 (2 × C), 38.6, 20.0, 19.9. ^{15}N NMR ($(CD_3)_2SO$, 600 MHz): δ = −79.3, −82.3, −206.2, −309.4.

2.2.4. 2-{(E, E)-4-[4-(dimethylamino)phenyl]buta-1,3-dien-1-yl}-3,5,8-trimethylbisthiazolo[4,5-e; 5,4-g]-1,3-benzothiazolium iodide (3b)

mp 275–277 °C. *Anal.*: Calcd. for $C_{24}H_{23}IN_4S_3\cdots 2/3\,CH_3OH$: C, 48.41; H, 4.23; N, 9.16; S, 15.72. Found: C, 47.95; H, 4.33; N, 9.12; S, 15.86. IR (powder film): ν = 3445 (—OH in CH_3OH, H-bonded), 3049 (=C—H, C_{Ar}—H), 2961 and 2921 and 2851 (C_{sp3}—H), 1615 and 1538 (C=C, C_{Ar}=C_{Ar}), 1471, 1416, 1366, 1261, 1103, 920, 821 cm^{-1}. ^{1}H NMR ($(CD_3)_2SO$, 600 MHz): δ = 8.13 (dd, *J* = 10.9 Hz, *J* = 14.4 Hz, 1H, CH=), 7.52 (d, *J* = 8.9 Hz, 2H, C_{Ar}—H), 7.41 (d, *J* = 15.0 Hz, 1H, CH=), 7.37 (d, *J* = 14.5 Hz, 1H, CH=), 7.24 (dd, *J* = 11.0 Hz, *J* = 14.9 Hz, 1H, CH=), 6.76 (d, *J* = 9.0 Hz, 2H, C_{Ar}—H), 4.77 (s, 3H, N^{+}—CH_3), 3.04 (s, 6H, N—$(CH_3)_2$), 3.03 (s, 3H, CH_3), 3.00 (s, 3H, CH_3). ^{13}C NMR ($(CD_3)_2SO$, 150.8 MHz): δ = 171.3, 168.9, 168.5, 152.1, 151.4, 148.3, 142.2, 138.1, 133.5, 130.5 (2 × C), 129.6, 126.1, 122.7, 122.2, 119.0, 112.0 (2 × C), 111.7, 39.6 (2 × C), 38.5, 20.0, 19.9. ^{15}N NMR ($(CD_3)_2SO$, 600 MHz): δ = −79.5, −82.5, −204.2, −317.3.

2.2.5. 2-{(E, E, E)-6-[4-(dimethylamino)phenyl]hexa-1,3,5-trien-1-yl}-trimethylbisthiazolo[4,5-e; 5,4-g]-1,3-benzothiazolium iodide (3c)

mp (the dark-green color changes to red by 212 °C) decomp. at 225 °C. *Anal.*: Calcd. for $C_{26}H_{25}IN_4S_3\cdots 3\,CH_3OH$: C, 48.87; H, 5.23; N, 7.86; S, 13.50. Found: C, 48.17; H, 4.57; N, 7.43; S, 13.13. IR

Table 1
Synthesis of final compounds.

Entry	Final compound	Temp. (°C)	Time (min)	Pressure (MPa)	Yield (%)
1	**3a**	110	30	0.60	78
2	**3b**	115	15	0.60	77
3	**3c**	115	40	0.62	28
4	**3d**	120	90	0.64	62
5	**3e**	120	70	0.67	45
6	**3f**	120	70	0.70	87

(powder film): ν = 3441 (—OH in CH_3OH, H-bonded), 3068 and 3035 (=C—H, C_{Ar}—H), 2957 and 2908 and 2851 (C_{sp3}—H), 2794, 2726, 2653, 1612 and 1574 (C=C, C_{Ar}=C_{Ar}), 1509, 1470, 1385, 1236, 1203, 1097, 998, 815 cm^{-1}. ^{1}H NMR ($(CD_3)_2SO$, 600 MHz): δ = 8.08 (dd, J = 11.1 Hz, J = 14.4 Hz, 1H, CH=), 7.45 (d, J = 8.9 Hz, 2H, C_{Ar}—H), 7.42 (d, J = 14.6 Hz, 1H, CH=), 7.32–7.27 (m, 1H, CH=), 7.03–7.02 (m, 2H, CH=), 6.81 (dd, J = 11.3 Hz, J = 14.1 Hz, 1H, CH=), 6.68 (d, J = 9.0 Hz, 2H, C_{Ar}—H), 4.78 (s, 3H, N^+—CH_3), 3.03 (s, 3H, CH_3), 3.00 (s, 3H, CH_3), 2.99 (s, 6H, N—$(CH_3)_2$). ^{13}C NMR ($(CD_3)_2SO$, 150.8 MHz): δ = 171.9, 169.5, 169.1, 151.7, 150.9, 149.9, 143.7, 142.7, 138.7, 134.1, 130.2, 130.0 (2 × C), 128.9, 126.8, 124.1, 124.0, 119.9, 113.5, 112.3 (2 × C), 40.2 (2 × C), 39.3, 20.6, 20.5. ^{15}N NMR ($(CD_3)_2SO$, 600 MHz): δ = −79.5, −82.4, −202.7, −322.4.

*2.2.6. 2-{(E)-2-[4-(diphenylamino)-phenyl]vinyl}-3,5,8-trimethylbisthiazolo[4,5-e; 5,4-g]-1,3-benzothiazolium iodide (**3d**)*

mp 187–190 °C. *Anal.*: Calcd. for $C_{32}H_{25}IN_4S_3\cdots 2/3\ CH_3OH$: C, 55.26; H, 3.93; N, 7.89; S, 13.55. Found: C, 55.09; H, 3.74; N, 7.88; S, 14.01. IR (powder film): ν = 3472 (—OH in CH_3OH, H-bonded), 3054 and 3032 and 3011 (=C—H and C_{Ar}—H), 2990 and 2965 and 2820 and 2904 (C_{sp3}—H), 2850, 2751, 2671, 2505, 1569 and 1545 and 1504 and 1485 (C=C, C_{Ar}=C_{Ar}), 1435, 1367, 1291, 1258, 1173, 1034, 946, 819, 700 cm^{-1}. ^{1}H NMR ($(CD_3)_2SO$, 600 MHz): δ = 8.29 (d, J = 15.5 Hz, 1H, CH=), 7.92 (d, J = 8.9 Hz, 2H, C_{Ar}—H), 7.82 (d, J = 15.5 Hz, 1H, CH=), 7.45 (t, J = 8.1 Hz, 4H, C_{Ar}—H), 7.27 (t, J = 7.4 Hz, 2H, C_{Ar}—H), 7.22 (d, J = 7.5 Hz, 4H, C_{Ar}—H), 6.92 (d, J = 8.8 Hz, 2H, C_{Ar}—H), 4.87 (s, 3H, N^+—CH_3), 3.03 (s, 3H, CH_3), 2.99 (s, 3H, CH_3). ^{13}C NMR ($(CD_3)_2SO$, 150.8 MHz): δ = 172.0, 170.8, 169.2, 152.0, 149.5, 145.8 (2 × C), 142.7, 138.8, 134.1, 132.4 (2 × C), 130.5 (4 × C), 130.2, 127.0, 126.7 (4 × C), 126.6, 126.1 (2 × C), 120.0, 119.2 (2 × C), 110.1, 39.7, 20.6, 20.5. ^{15}N NMR ($(CD_3)_2SO$, 600 MHz): δ = −79.6, −82.4, −199.9, −269.7.

*2.2.7. 2-{(E, E)-4-[4-(diphenylamino)phenyl]buta-1,3-dien-1-yl}-3,5,8-trimethylbisthiazolo[4,5-e; 5,4-g]-1,3-benzothiazolium iodide (**3e**)*

mp 178–181 °C. *Anal.*: Calcd. for $C_{34}H_{27}IN_4S_3\cdots 2/3\ CH_3OH$: C, 56.57; H, 4.06; N, 7.61; S, 13.07. Found: C, 56.21; H, 3.78; N, 7.43; S, 13.24. IR (powder film): ν = 3479 and 3407 (—OH in CH_3OH, H-bonded), 3054 and 3031 (=C—H and C_{Ar}—H), 2966 and 2920 (C_{sp3}—H), 2692, 2632, 2555, 2309, 2004, 1540 and 1506 and 1475 (C=C, C_{Ar}=C_{Ar}), 1406, 1331, 1300, 1262, 1150, 1099, 999, 945, 831, 698 cm^{-1}. ^{1}H NMR ($(CD_3)_2SO$, 600 MHz): δ = 8.17 (dd, J = 10.6 Hz, J = 14.6 Hz, 1H, CH=), 7.56 (d, J = 8.8 Hz, 2H, C_{Ar}—H), 7.55 (d, J = 14.7 Hz, 1H, CH=), 7.42–7.40 (m, 4H, C_{Ar}—H), 7.40 (d, J = 15.9 Hz, 1H, CH=), 7.31 (dd, J = 10.5 Hz, J = 15.2 Hz, 1H, CH=), 7.21–7.18 (m, 2H, C_{Ar}—H), 7.16–7.14 (m, 4H, C_{Ar}—H), 6.92 (d, J = 8.8 Hz, 2H, C_{Ar}—H), 4.81 (s, 3H, N^+—CH_3), 3.03 (s, 3H, CH_3), 3.00 (s, 3H, CH_3). ^{13}C NMR ($(CD_3)_2SO$, 150.8 MHz): δ = 172.1, 169.8, 169.3, 150.9, 150.2, 146.5, 146.4 (2 × C), 142.7, 138.8, 134.1, 130.38, 130.35 (4 × C), 130.3 (2 × C), 128.4, 127.1, 126.1 (4 × C), 125.4, 125.3 (2 × C), 120.8 (2 × C), 120.2, 114.9, 39.5, 20.6, 20.5. ^{15}N NMR ($(CD_3)_2SO$, 600 MHz): δ = −79.6, −82.5, −200.0, −273.7.

2.2.8. 2-[(E)-2-(9-julolidinyl)vinyl]-3,5,8-trimethylbisthiazolo[4,5-e; 5,4-g]-1,3-benzothiazolium iodide (3f)

mp 225–228 °C. *Anal.*: Calcd. for $C_{26}H_{25}IN_4S_3 \cdot 1/2\ CH_3OH$: C, 50.31; H, 4.30; N, 8.86; S, 15.21. Found: C, 50.04; H, 4.05; N, 8.90; S, 15.71. IR (powder film): ν = 3444 (—OH in CH_3OH, H-bonded), 3044 and 3001 (=C—H and C_{Ar}—H), 2923 and 2837 (C_{sp3}—H), 2710, 1621 and 1566 and 1520 (C=C, C_{Ar}=C_{Ar}), 1481, 1433, 1410, 1315, 1232, 1208, 1147, 1104, 907, 822 cm^{-1}. ^{1}H NMR ($(CD_3)_2SO$, 600 MHz): δ = 7.96 (d, J = 14.9 Hz, 1H, CH=), 7.47 (s, 2H, C_{Ar}—H), 7.41 (d, J = 14.9 Hz, 1H, CH=), 4.71 (s, 3H, N^+—CH_3), 3.37 (t, J = 5.5 Hz, 4H, CH_2), 3.00 (s, 3H, CH_3), 2.97 (s, 3H, CH_3), 2.70 (t, J = 6.0 Hz, 4H, CH_2), 1.91–1.87 (m, 4H, CH_2). ^{13}C NMR ($(CD_3)_2SO$, 150.8 MHz): δ = 171.6, 169.4, 168.6, 150.6, 148.5, 142.8, 138.3, 133.8, 131.1 (2 × C, very weak signal), 129.6, 125.7, 121.7, 121.3 (2 × C), 118.4, 104.1, 50.2 (2 × C), 38.7, 27.3 (2 × C), 21.0 (2 × C), 20.6, 20.4. ^{15}N NMR (DMSO, 600 MHz): δ = −79.3, −82.3, −211.4, −287.0.

2.2.9. 2-[(E)-2-(9-julolidinyl)vinyl]-3-methylbenzothiazolium iodide (7f)

To the solution of 2,3-dimethylbenzothiazolium iodide (0.87 g, 0.003 mol) in methanol (15 mL), 9-julolidinyl)carbaldehyde (0.6 g, 0.003 mol) and a few drops of pyridine were added. The reaction mixture was heated to reflux for 12 h. The dark precipitate with metallic lustre was filtered off and washed with diethyl ether. Yield: 1.2 g (85%); mp 233–234 °C. IR (powder film): ν = 3425 (—OH in CH_3OH, H-bonded), 3058 and 3012 (=C—H, C_{Ar}—H), 2933 and 2841 and 2706 and 2609 (C_{sp3}—H), 1617 and 1569 (C=C, C_{Ar}=C_{Ar}), 1518, 1494, 1453, 1315, 1293, 1157 cm^{-1}. ^{1}H NMR ($(CD_3)_2SO$, 600 MHz): δ = 8.23 (d, J = 7.8 Hz, 1H, C_{Ar}—H), 8.01 (d, J = 7.8 Hz, 1H, C_{Ar}—H), 7.88 (d, J = 15.0 Hz, 1H, CH=), 7.74 (dt, J = 7.8 Hz, J = 0.9 Hz, 1H, C_{Ar}—H), 7.63 (dt, J = 7.8 Hz, J = 0.9 Hz, 1H, C_{Ar}—H), 7.44 (d, J = 15.0 Hz, 1H, CH=), 4.16 (s, 3H, N^+—CH_3), 3.37 (t, J = 5.9 Hz, 4H, CH_2), 2.73 (t, J = 5.8 Hz, 4H, CH_2), 1.92–1.88 (m, 4H, CH_2). ^{13}C NMR ($(CD_3)_2SO$, 150.8 MHz): δ = 170.8, 150.6, 148.3, 142.4, 130.8 (2 × C, weak signal) 129.1, 127.4, 126.9, 124.1, 121.6, 121.0 (2 × C), 115.9, 104.6, 50.1 (2 × C), 35.6, 27.4 (2 × C), 21.1 (2 × C). ^{15}N NMR ($(CD_3)_2SO$, 600 MHz): δ = −212.2, −289.4.

2.2.10. Quaternization with dimethyl sulfate

Compound **1** (0.03 g, 0.1 mmol) was partly dissolved in toluene (3 mL). Dimethyl sulfate (0.29 mL, 0.003 mol, 30 eq.) was added and the reaction mixture was heated at 110 °C for 8 h. Toluene was evaporated under vacuum and the crude product was washed several times with diethyl ether. The composition of the product was established by ^{1}H NMR and is discussed below (Sections 3.1 and 3.3).

2.2.11. Quaternization with trimethyloxonium tetrafluoroborate

In a glass vessel for microwave reactor the compound **1** (0.1 g, 0.34 mmol) was dissolved in dried 1,2-dichloroethane (5 mL). Trimethyloxonium tetrafluoroborate (0.251 g, 1.7 mmol, 5 eq.) was added and the reaction mixture, under inert atmosphere, was exposed to microwave irradiation for 5 × 10 min at 165 °C. The brownish precipitate was filtered off and the composition of the crude product (0.156 g) was established by ^{1}H NMR and is discussed below (Sections 3.1 and 3.3).

2.2.12. Quaternization with 1,3-propanesultone

Compound **1** (0.05 g, 0.17 mmol) was dissolved in toluene (2 mL) and 1,3-propanesultone (0.060 mL, 0.68 mmol, 4 eq.) was added. The reaction mixture was heated at 110 °C for 19 h. The white precipitate was filtered off and washed with diethyl ether. The composition of the crude product (0.055 g) was established by ^{1}H NMR.

*2.2.13. ^{1}H NMR for 3-(2,5,8-trimethylbisthiazolo[4,5-e; 4,5-g]-1,3-benzothiazolium-3-yl)propane-1-sulfonate (**6a**) and for 3-(2,5,8-trimethylbisthiazolo[4,5-e; 5,4-g]-1,3-benzothiazolium-3-yl)propane-1-sulfonate (**6b**)*

Minor isomer: (CD_3OD, 300 MHz): δ = 5.61–5.57 (m, 2H, N^+—CH_2—), 3.35 (s, 3H, CH_3), 3.12 (t, J = 7.0 Hz, 2H, CH_2), 3.062 (s, 3H, CH_3), 3.002 (s, 3H, CH_3), 2.56–2.46 (m, 2H, CH_2).

Table 2
Calculated quantum chemical descriptors related to nonlinear optical properties of studied benzothiazolium cations: energy difference gap between HOMO and LUMO orbitals (ΔE), bond length alternation index (BLA), polarizability α, first and second hyperpolarizabilities β and γ.

Compound	ΔE (eV)	BLA (Å)	α ($\times 10^{-24}$ esu)	β ($\times 10^{-30}$ esu)	γ ($\times 10^{-36}$ esu)
3a	2.64	0.043	138	230	217
3b	2.36	0.0325	183	427	119
3c	2.06	0.027	240	667	1181
3d	2.41	0.0425	184	341	667
3e	2.13	0.032	233	657	564
3f	2.53	0.036	153	236	91

Major isomer: (CD_3OD, 300 MHz): $\delta = 5.59–5.53$ (m, 2H, $N^+—CH_2—$), 3.36 (s, 3H, CH_3), 3.12 (t, $J = 7.0$ Hz, 2H, CH_2), 3.055 (s, 3H, CH_3), 2.995 (s, 3H, CH_3), 2.56–2.46 (m, 2H, CH_2).

2.3. X-ray data collection, structure solution and refinement

The green crystal of the compound **2b** was mounted on a cactus thorn by epoxy glue. Measurement was taken on an Oxford Diffraction Gemini R κ-axis diffractometer [20] with a graphite-monochromated Mo Kα radiation ($\lambda = 0.71073$ Å) at room temperature (293 K) using ω scans. Corrections for Lorentz, polarization and absorption effects were applied using the CrysAlisPro software [20]. The structure was solved by structure-invariant direct methods using VLD procedure in SIR-2011 [21] and refined using SHELXL-97 [22]. Molecular graphic employed include DIAMOND [23] and Mercury [24]. The crystal data and details of data collection and refinement are given in Table 3.

All non-H atoms were refined anisotropically as free atoms. The hydrogen atoms were refined by using the riding model with SHELXL-default d(C—H) values. C10, C13 and C20 methyl groups were refined with staggered geometry, C11 and C12 methyl groups were refined as disordered (freely rotating). H1 atom was refined as follows: y coordinate was fixed to 0.25 and bond lengths d(H1—O1) and d(H1—C20) were restrained to 0.82(1) Å and 1.41(1) Å to obtain reasonable geometry. Thermal parameters of the H atoms were set to $U_{iso}(H) = 1.5\ U_{eq}(C, O)$.

2.4. Computational details

The optimal geometries for each compound *in vacuo* were calculated in the Turbomole 6.2 program [25], using the DFT method [26] and the B3LYP exchange–correlation functional [27]. On all atoms the TZVP basis set [28] was employed. For calculating the ESP charges a parametrization very close to that by Singh and Kollman [29] was used. The time dependent DFT method [30] was used to calculate the first excited state.

First order hyperpolarizabilities (β) [31] were calculated using the method PM3 [32] from the program package Ampac 8 [33].

3. Results and discussion

3.1. Synthesis and calculations

The six step synthesis of the unsymmetrical trimethylbenzotristhiazole (BTT) we reported recently [14] (Scheme 4).

To enhance the electron withdrawing character of the benzotristhiazole building block we have tried to methylate the heterocyclic nitrogens. Firstly we have performed the quantum chemical calculations of the starting trimethylbenzotristhiazole (**1**) and monomethylated products by DFT methods. The atom centered ESP charges on nitrogen atoms were used as a measure of nucleophilicity (Fig. 1). According to the calculations the methylation of the nitrogen in b-ring (*N-b*) is preferred to *N-a*. The least charge density was calculated on *N-c*.

DFT total energy values of methylated cations can serve for comparison of the thermodynamic stability of possible monomethylated products. Values of relative energies are presented in Fig. 2. The cation methylated on *N-b* shows the least value of energy, the product of methylation on *N-a* is slightly higher in energy and the third isomer methylated on *N-c* is least probable to be formed. As a conclusion of quantum chemical calculations we

Table 3
Experimental data for **2b**.

Empirical formula	$C_{14}H_{16}IN_3OS_3$
M_r	465.38
Crystal system, space group	orthorhombic, *Pnma*
Unit cell dimensions	Determined from 7684 reflections
a (Å), α (°)	24.1828 (6), 90
b (Å), β (°)	6.8113 (1), 90
c (Å), γ (°)	10.7365 (3), 90
V (Å^3)	1768.47 (7)
Z, density (calcd.) (g cm^{-3})	4, 1.748
μ	2.159 mm^{-1}
F(000)	920
Absorption correction, T_{min}, T_{max}	Analytical, 0.551, 0.916
Crystal size (mm)	0.88 × 0.18 × 0.04
Crystal habit, color	Plate, green
θ Range for data collection (°)	3.5–29.5
Limiting indices	$h = -31 \rightarrow 32$
	$k = -9 \rightarrow 8$
	$l = -14 \rightarrow 13$
Reflections collected/unique/observed[$I > 2\sigma(I)$]	28599/2526/1916 [$R_{int} = 0.028$]
Completeness to θ (°)	99.0% to 28.5°
Data/restraints/parameters	2526/2/135
Final weighting scheme	$w = 1/[\sigma^2(F_o^2) + (0.0397P)^2 + 1.1107P]$ where $P = (F_o^2 + 2F_c^2)/3$
S/restrained S	1.084/1.084
Final R indices [$I > 2\sigma(I)$]	$R = 3.63\%$, $wR = 8.10\%$
Final R indices (all data)	$R = 5.57\%$, $wR = 8.88\%$
Largest difference peak/hole (e Å^{-3})	0.64/−0.91

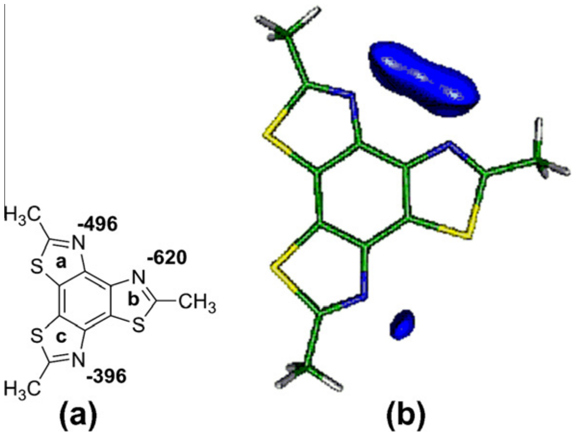

Fig. 1. (a) Calculated ESP charges ($Q \times 10^3$ values are presented) on nitrogens of starting neutral compound BTT. (b) MEP visualization of the computed nitrogen electron densities.

can predict the probability of formation of monomethylated products: **cat_b** > **cat_a** ≫ **cat_c**.

The structure of dimethylated salts can be also predicted based on calculated total energy values of isomers. The results shown in Fig. 2 represent relative energy values of the three conceivable dications. It is possible to exclude the isomer **dicat_ab** due to the repulsion of neighboring methyl groups and repulsion of quite near positive charges on nitrogens *N-a* and *N-b*. The isomers **dicat_ac** and **dicat_bc** are much more likely to be formed as could be also seen from the MEP visualization of the computed nitrogen electron densities (Fig. 3). The highest electron density is on the *N-c*.

The quaternization reactions were realized with several alkylating agents:

(1) Alkylation of BTT with an excess of methyl iodide in methanol ran with a high conversion and produced a mixture of two monomethylated salts. The solid product which precipitated from the reaction mixture consisted of the isomeric salts **2a** and **2b** (Scheme 1) in a ratio of 3:7. The opposite ratio of monomethylated products (7:3) was determined in the filtrate. To summarize the results we have taken into account the amount of the precipitate (59%) and that of the filtrate (41%). The final ratio of monomethylated products was 46:54, roughly 1:1. The precipitate was further treated and the prevailing isomer (**2b**) was separated by crystallization. Its right structure was proved by X-ray analysis. A further quaternization either of the mixtures **2a** and **2b** or of the pure isomer **2b** with dimethyl sulfate or with trimethyloxonium tetrafluoroborate gave the dimethylated products only in a yield of 10%.

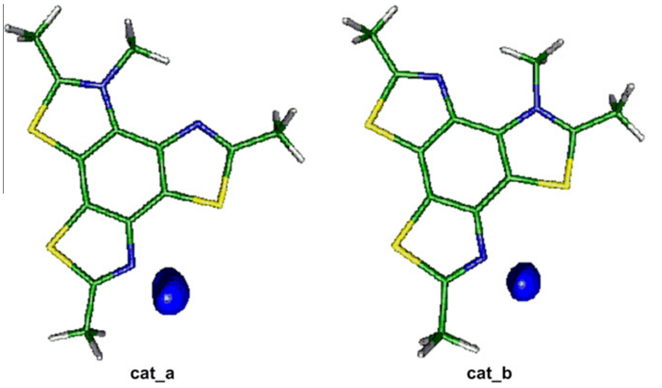

Fig. 3. MEP visualization of the computed nitrogen electron densities for **cat_a** and **cat_b**.

(2) Methylation with dimethyl sulfate (Scheme 2, option **A**) offered a mixture of mono- (13%) and dimethylated salts (78%). The two monomethyl isomers (**4a** and **4b**) were formed in a ratio of 2:3 and the two dimethyl isomers (**4c** and **4d**) were formed in a ratio of 1.15:1. A small amount (9%) of the starting compound was also observed.

(3) Trimethyloxonium tetrafluoroborate is known as a powerful alkylating agent (Scheme 2, option **B**). With the 5-fold excess of $(CH_3)_3\ O^+\ BF_4^-$ we have obtained a mixture of monomethylated isomers (53%), dimethylated isomers (37%) and 10% of untreated starting BTT. The two monomethyl isomers (**5a** and **5b**) as well as the two dimethyl isomers (**5c** and **5d**) have been formed in a ratio of 1:1. A further quaternization of the crude product with another 3-fold excess of $(CH_3)_3\ O^+$ BF_4^- have not changed the composition of the mixture.

(4) A mixture of two monoalkylated products in a ratio of 65:35 has been obtained using excess of 1,3-propanesultone as an alkylating reagent (Scheme 3). Which of the two isomers is the major one, we deduced from the calculated total energies and by comparing the ^{1}H NMR spectrum with those of **cat_a** and **cat_b**. According to the relative total energies given in Fig. 4 the isomer **6b** is slightly preferred. Comparing the ^{1}H NMR shifts for the methyl group bound to the carbon in the alkylated ring with the corresponding one in **cat_a** resp. **cat_b**, we can see that the one for **cat_a** ($\delta = 3.269$) and the minor isomer ($\delta = 3.35$) are lower shifted than that for **cat_b** ($\delta = 3.292$) and the major isomer ($\delta = 3.36$). Similar shifts can be observed for the CH_2 groups bound directly to the nitrogen and the corresponding methyl groups in cations. The signals for **cat_a** ($\delta = 4.808$) and the minor isomer ($\delta = 5.61–5.57$) are higher shifted than that for **cat_b** ($\delta = 4.803$) and the major isomer ($\delta = 5.59–5.53$). So we can conclude that the major isomer could be compound **6b**.

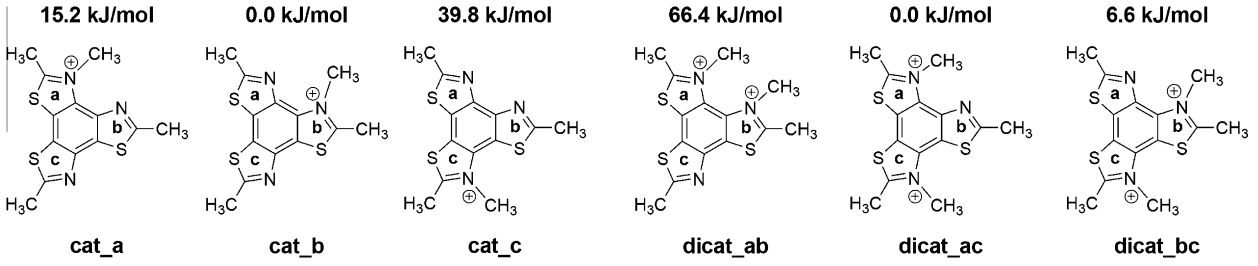

Fig. 2. Calculated relative energies of the three possible monomethylated cations (**cat_a**, **cat_b**, **cat_c**) and three possible dimethylated cations (**dicat_ab**, **dicat_ac**, **dicat_bc**).

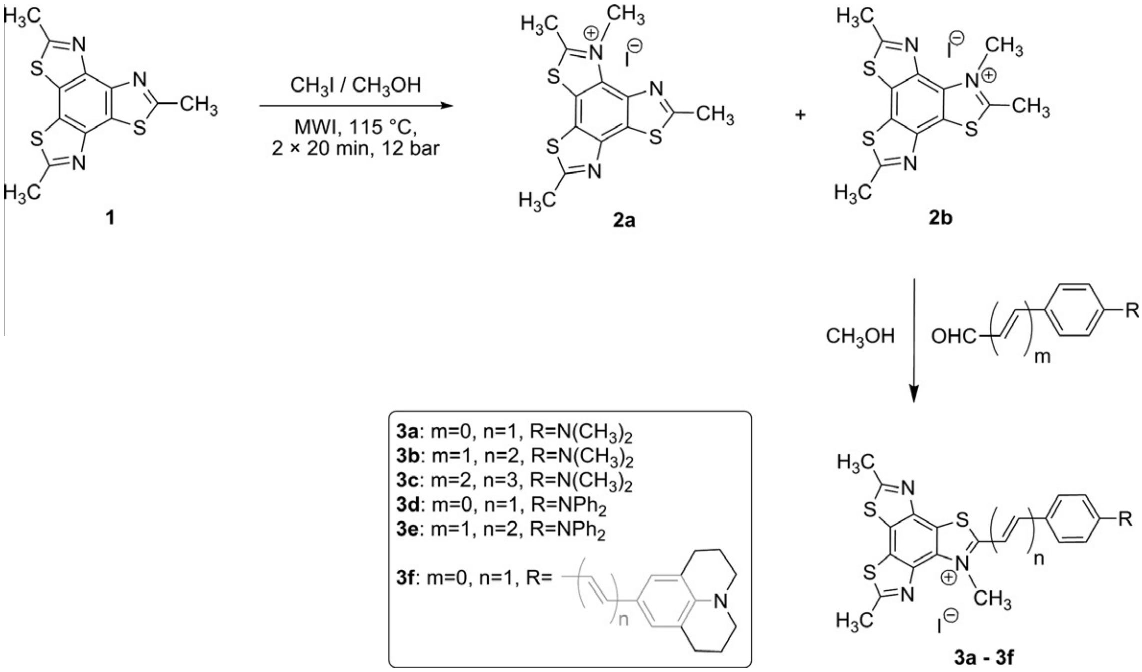

Scheme 1. The synthesis of final products.

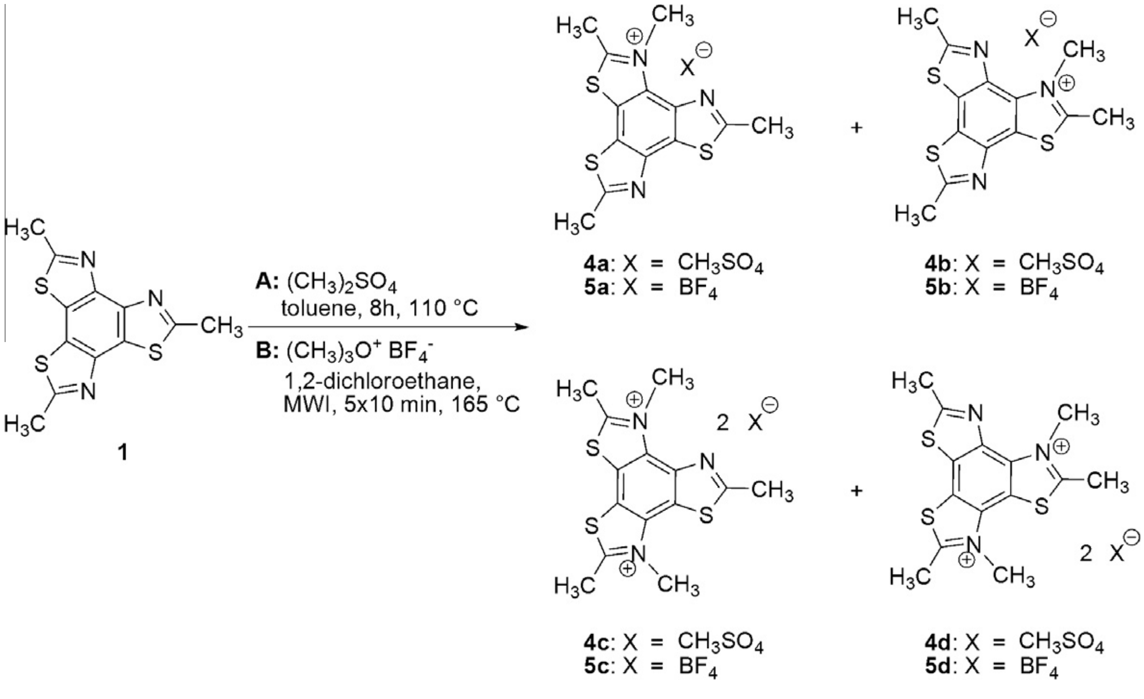

Scheme 2. Methylation of **1** with (A) dimethyl sulfate (products **4a**–**4d**); (B) trimethyloxonium tetrafluoroborate (products **5a**–**5d**).

We performed the reaction with 1,3-propanesultone to obtain a salt with a better solubility. The mixture of isomers **6a** and **6b** is very well soluble in methanol, but insoluble in DMSO whereas the previous methylated compounds dissolve reversely.

The last step in the synthesis of the final compounds **3a**–**3f** is the Knoevenagel reaction of **2b** with aromatic aldehydes containing an electron-releasing group (Scheme 1). These reactions are performed under microwave irradiation which shortens the reaction time and the obtained yields are very good (Table 1). Similarly to the compound **2b** (that was confirmed by X-ray analysis) we presume that compounds **3a**–**3f** contain in their crystalline structure molecules of methanol. It can be seen in the ^{1}H NMR spectra and IR spectra (strong signals for —OH hydrogen bonds). Even drying the compounds under high vacuum for 8 h does not remove the methanol from the crystalline structure.

Calculated quantum-chemical descriptors related to the nonlinear properties of studied cations are reported in Table 2. Small HOMO–LUMO energy gap (ΔE) predicts interesting first hyperpolarizability β as can be seen in compounds **3c** and **3e**. The BLA index represents the measure of conjugation and the smallest values are

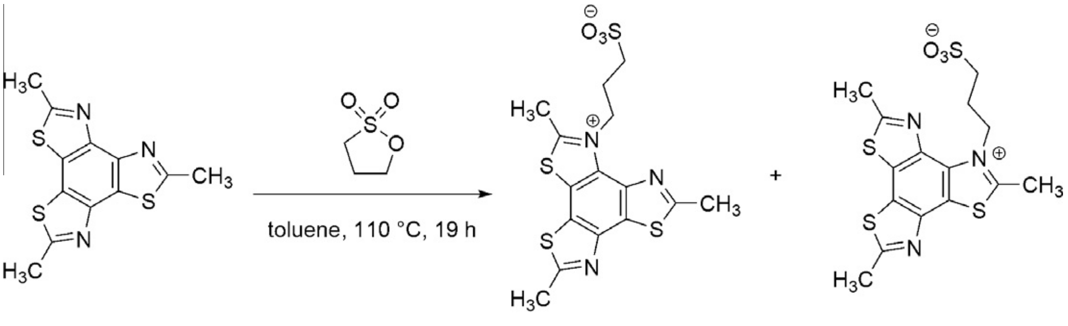

6a **6b**

Scheme 3. Reaction with 1,3-propanesultone.

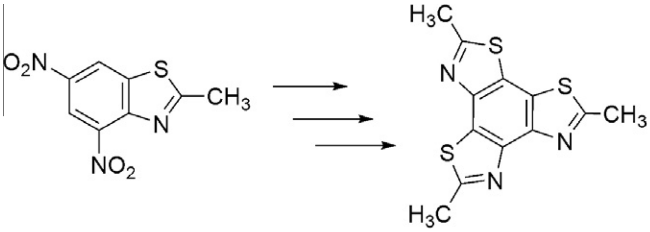

Scheme 4. Trimethylbenzotristhiazole.

again observed in cations **3c** and **3e.** These cations are also characterized by the highest values of linear polarizability α. The most important parameters are hyperpolarizabilities β and γ, which predict the structures with possible application in nonlinear optics. As can be seen from Table 2 hyperpolarizability β is influenced by the number of double bonds in the conjugated bridge. The exchange of the electrondonor NMe_2 for NPh_2 group causes a significant increase in the β values (**3a** → **3d, 3b** → **3e**). The β values for **3c** and **3e** seem to be quite promising. Even if a direct relation between second hyperpolarizability γ and structural units of studied cations is not so evident, the unexpected high value of γ for **3c** was surprising and encouraging. Based on these findings we have combined the best structural units: three double bonds and diphenylamino donor substituent to design and calculate the new predicted cation. Its structure can be deduced from Scheme 1: compound **3**, with $n = 3$, R = NPh_2. The calculations fulfilled our expectation: the predicted structure has a minimal HOMO–LUMO energy gap ($\Delta E = 1.91$ eV), polarizability $\alpha = 294 \times 10^{-24}$ esu and excellent first hyperpolarizability ($\beta = 1012 \times 10^{-30}$ esu).

Further properties of compounds **3a**–**3f** are discussed in Section 3.4 of this article.

3.2. X-ray crystal structure of compound *2b*

The crystal of the compound **2b** was obtained by slow evaporation of methanol solution at room temperature. Title compound crystallizes as crystallosolvate with methanol (molar ratio 1:1) in orthorhombic *Pnma* space group with unit cell parameters $a = 24.1828$ (6) Å, $b = 6.8113$ (1) Å, $c = 10.7365$ (3) Å, $V = 1768.47$ (7) $Å^3$ and $Z = 4$. The crystal structure of **2b** is given in Fig. 5 and packing pattern is given in Fig. 6. Selected geometry features are given in Table 5.

2,3,5,8-tetramethylbisthiazolo[4,5-e; 5,4-g]-1,3-benzothiazolium cation, iodide anion and methanol molecule are located on mirror planes of unit cell. Cation contains weak intramolecular C13—H13A···N2 bond (Table 4). Intermolecular interactions consist of π–π stacking interactions between cations lying in neighboring mirror planes and of hydrogen bonding network containing both intraplanar and interplanar interactions. Intraplanar are stronger of them: *d*(H···A) is more than 0.5 Å shorter than sum of VdW radii for O1—H1···I1 and more than 0.2 Å shorter for C10—H10A···I1 interaction. Interplanar interactions are based on crystallographically equivalent C10—H10B/C···I1, which are somewhat weaker than interplanar C—H···I interaction. (All *d*(H···A) distances discussed here are based of constrained H-atoms positions for X-ray data, real distances are even shorter [34].)

As can be seen from the Table 5, the calculated values correspond very well with the experimental. The differences in C—C bonds are only 0.002–0.016 Å and in C—N bonds only 0.002–0.008 Å. Exception is the bond C13—N1, where the differ-

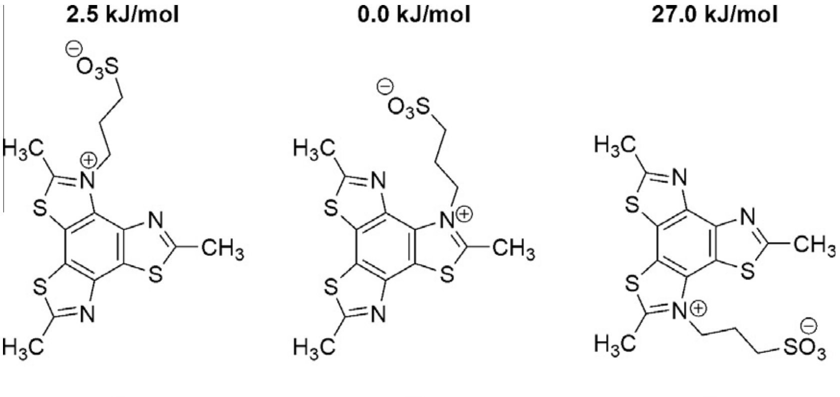

6a **6b** **6c**

Fig. 4. The relative total energies for the isomers **6a**, **6b** and **6c**.

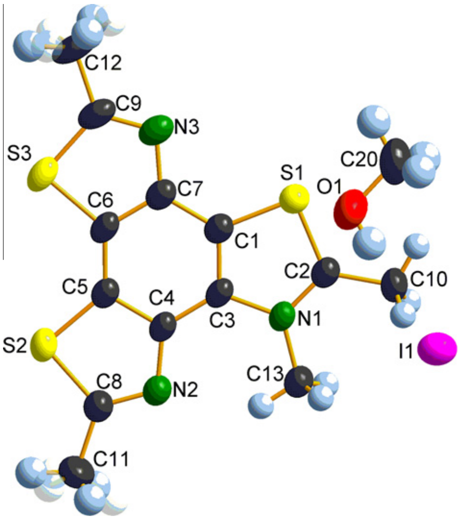

Fig. 5. Crystal structure of compound **2b** with numbering scheme. All non-hydrogen atoms are drawn as 50% probability ellipsoids; H atoms are drawn as spheres of arbitrary small radius for clarity.

ence is 0.038 Å. The largest differences are in C—S bonds (0.014–0.053 Å). Comparing the values for the angles, we can see that the differences are in the range 0–2.5°. The computed dihedral angles show, that the structure is planar which was also confirmed by the experiment.

3.3. NMR spectroscopy

The prepared monomethylated and dimethylated salts except the compound **2b**, which structure was fully determined by X-ray, were identified by ^1H NMR spectroscopy. The values for each cation are given in the following. The shifts are not dependent on the counterion. To determine which signals belong to **dicat_ac** and which to **dicat_bc** we performed a reaction, where we further quaternized compound **2b** with dimethyl sulfate. According to ^1H NMR a yield of approximately 30% was estimated, but we could precisely assign the signals belonging to **dicat_bc**.

cat_a ^1H NMR ($(CD_3)_2SO$, 300 MHz): $\delta = 4.808$ (s, 3H, N^+—CH_3), 3.269 (s, 3H, CH_3), 3.060 (s, 3H, CH_3), 3.006 (s, 3H, CH_3).
cat_b ^1H NMR ($(CD_3)_2SO$, 300 MHz): $\delta = 4.803$ (s, 3H, N^+—CH_3), 3.292 (s, 3H, CH_3), 3.054 (s, 3H, CH_3), 3.010 (s, 3H, CH_3).
dicat_ac ^1H NMR ($(CD_3)_2SO$, 300 MHz): $\delta = 4.820$ (s, 3H, N^+—CH_3), 4.502 (s, 3H, N^+—CH_3), 3.341 (s, 3H, CH_3), 3.325 (s, 3H, CH_3), 3.155 (s, 3H, CH_3).
dicat_bc ^1H NMR ($(CD_3)_2SO$, 300 MHz): $\delta = 4.872$ (s, 3H, N^+—CH_3), 4.585 (s, 3H, N^+—CH_3), 3.378 (s, 3H, CH_3), 3.357 (s, 3H, CH_3), 3.125 (s, 3H, CH_3).

Table 4
Hydrogen bonding interactions in the structure of **2b** (Å, °).

D—H···*A*	*D*—H	H···*A*	*D*···*A*	*D*—H···*A*
Intramolecular				
C13—H13*A*···N2	0.96	2.21	3.001 (5)	139
Intermolecular–intraplanar				
O1—H1···I1	0.82 (1)	2.67 (1)	3.488 (4)	176 (2)
C10—H10*A*···I1[a]	0.96	2.97	3.932 (4)	178
Intermolecular–interplanar				
C10—H10*B*···I1	0.96	3.05	4.001 (2)	173
C10—H10*C*···I1[b]	0.96	3.05	4.001 (2)	173

Symmetry codes:
[a] $-x + 1/2, -y + 1, z + ½$.
[b] $x, y + 1, z$.

^{15}N NMR spectra of compounds **3a**–**3f** show that the signals for neutral nitrogens from the benzotristhiazolium core are always shifted around −80 ppm. Signals for the quaternized nitrogens can be found from −199.9 ppm to −211.4 ppm. The shifts for the nitrogens from —NMe_2 and —NPh_2 groups or julolidine moiety vary from −269.7 ppm to −322.4 ppm.

3.4. UV–Vis and emission spectroscopy

The UV–Vis absorption and emission characteristics of the target salts **3a**–**3f** are presented in Table 6. The compounds under study absorb in the visible region and are characterized by a strong long wave ICT band with molar absorption coefficient of about 50,000–100,000 M^{-1} cm^{-1}. The high value of the molar absorption coefficient indicates an extensive conjugation of π-electrons suggesting a planar structure of the molecule in its ground state.

The results can be compared to those of the corresponding one dimensional benzothiazolium salts **7a**–**7f** (Fig. 7) with push–pull structure, which have been published by our group [18,35].

The two thiazole cycles in salts **3a**–**3f** could be understood as auxiliary units enhancing the electron withdrawing capacity of the benzothiazolium moiety. This structural motif results in the red shift of the long wave absorption band as well as in higher values of extinction coefficients ε compared to the corresponding linear structures. The comparison of λ_A values for salts **7a**–**7f** and the corresponding neutral benzothiazoles [35] indicates that the quaternary nitrogen in benzothiazolium core shows a serious influence on the high withdrawing character of the benzothiazolium unit (high bathochromic shift) compared to the corresponding neutral benzothiazoles.

The expected bathochromic shift was also observed by prolongation of the π-bridge connecting the donor and the acceptor parts of studied compounds. The exchange of NMe_2 substituent for NPh_2 caused a hypsochromic shift of long wave band as well as reduction of extinction coefficients, probably owing to lower planarity of the system [18]. On the contrary, the julolidine donor substitu-

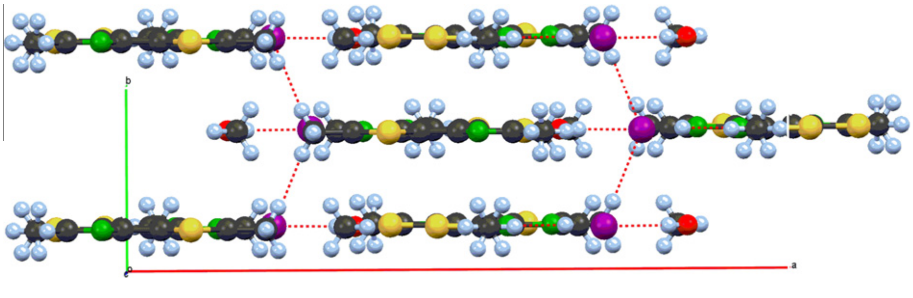

Fig. 6. View of the cell packing along the *c* axis. Dashed lines indicate the hydrogen bonding interactions.

Table 5
Selected geometry features of compound **2b**.

Parameters Bond lengths (Å)	Calculated	Experimental	Parameters Angles (°)	Calculated	Experimental
C1—C3	1.395	1.382 (5)	C3—C1—C7	122.1	120.8 (3)
C1—C7	1.402	1.417 (5)	C1—C3—C4	119.7	121.1 (3)
C1—S1	1.748	1.726 (4)	C5—C4—C3	118.1	118.1 (3)
C2—N1	1.330	1.322 (5)	C4—C5—C6	121.5	120.7 (3)
C2—C10	1.487	1.474 (5)	C7—C6—C5	120.2	120.8 (3)
C2—S1	1.719	1.705 (4)	C6—C7—C1	118.4	118.5 (3)
C3—C4	1.418	1.409 (5)	N1—C2—S1	113.1	113.3 (3)
C3—N1	1.404	1.410 (4)	C10—C2—S1	122.8	122.5 (3)
C4—N2	1.376	1.372 (5)	N1—C2—C10	124.2	124.2 (3)
C4—C5	1.409	1.407 (5)	N2—C8—S2	114.6	115.7 (3)
C5—C6	1.401	1.408 (5)	C11—C8—S2	120.5	120.4 (3)
C5—S2	1.747	1.724 (4)	N2—C8—C11	124.9	123.9 (4)
C6—C7	1.404	1.388 (5)	N3—C9—S3	114.7	116.4 (3)
C6—S3	1.747	1.730 (3)	C12—C9—S3	120.3	120.2 (4)
C7—N3	1.372	1.382 (5)	N3—C9—C12	125.1	123.4 (4)
C8—N2	1.294	1.292 (5)	C2—N1—C3	114.3	113.8 (3)
C8—C11	1.490	1.497 (6)	C2—N1—C13	121.5	121.9 (3)
C8—S2	1.780	1.741 (4)	C3—N1—C13	124.2	124.2 (3)
C9—N3	1.292	1.296 (5)	C8—N2—C4	112.2	110.9 (3)
C9—C12	1.489	1.498 (6)	C9—N3—C7	111.6	109.1 (3)
C9—S3	1.792	1.739 (5)	C2—S1—C1	90.33	90.35 (18)
C13—N1	1.480	1.442 (5)	C5—S2—C8	88.85	89.28 (18)
			C6—S3—C9	88.63	89.26 (19)
Dihedral angles (°)					
C10—C2—N1—C3	−179.8	180.0	C11—C8—N2—C4	179.9	180.0
C10—C2—N1—C13	1.17	0.0	C11—C8—S2—C5	180.0	180.0
S1—C2—N1—C13	−179.1	180.0	C12—C9—N3—C7	−179.9	180.0
C1—C3—N1—C13	179.2	180.0	C12—C9—S3—C6	179.9	180.0
C10—C2—S1—C1	179.7	180.0			

Table 6
λ_A – Absorption maximum, λ_F – fluorescence maximum, ε – molar absorption coefficient, $\nu_A - \nu_F$ – Stokes shift, Φ_F – fluorescence quantum yield. Used solvent: methanol.

Compound	λ_A (nm)	ε (M^{-1} m^{-1})	Compound	λ_A (nm)	ε (M^{-1} cm^{-1})	λ_F (nm)	$\nu_A - \nu_F$ (nm)	Φ_F
7a	523	62,400	**3a**	540	63,800	612	72	0.011
7b	562	58,200	**3b**	580	76,300	718	138	0.039
7c	580	46,300	**3c**	598	54,300	832	234	0.105
7d	512	36,800	**3d**	528	53,900	710	182	0.0023
7e	537	52,800	**3e**	550	52,600	782	232	0.0035
7f	567	10,1000	**3f**	586	98,000	635	49	0.0072

ent causes extraordinary red shift with the highest extinction coefficient. Unlike the —NMe_2 and —NPh_2 donors, the nitrogen in julolidine substituent is rigidized and rehybridized from pyramidal to planar configuration. This structure enables better conjugation and more effective charge transfer. For comparison we have also prepared the corresponding linear benzothiazolium salt **7f** with julolidine donor, which confirmed the observed trends.

The effective charge transfer in benzothiazolium cations **3a**–**3f** and **7a**–**7f** enables a good overlap between the squares of the vibrational wave functions of the initial and final electronic states which results in limited emission (rapid radiationless transfer). Observed low fluorescence quantum yield values (Φ_F) for **3a**–**3f** and **7a**–**7f** [18] confirmed this result. The Φ_F values for **3a**–**3e** are enhanced with increasing conjugation length of the chromophoric system. We assume that this behavior is associated with the rotation around the C—C single bonds in conjugated bridge (i.e. intramolecular twisting) [36]. Enhanced conjugation leads to an increase in the electron density distribution of the C—C single bonds. The higher electron density distribution of C—C single bonds hinders the twisting of these bonds and therefore results

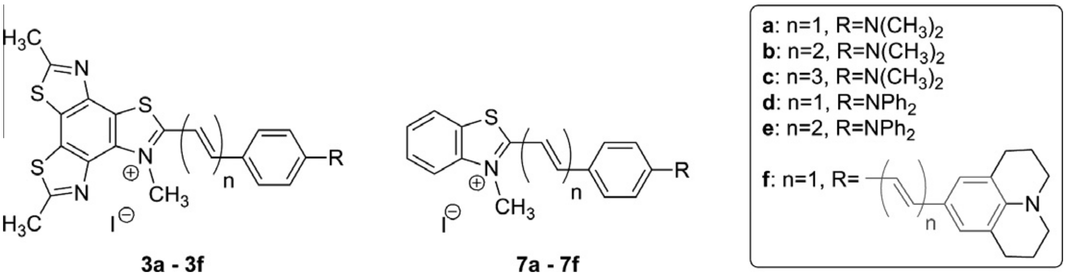

3a - 3f **7a - 7f**

Fig. 7. Comparison of final structures (**3a**–**3f**) with linear compounds (**7a**–**7f**).

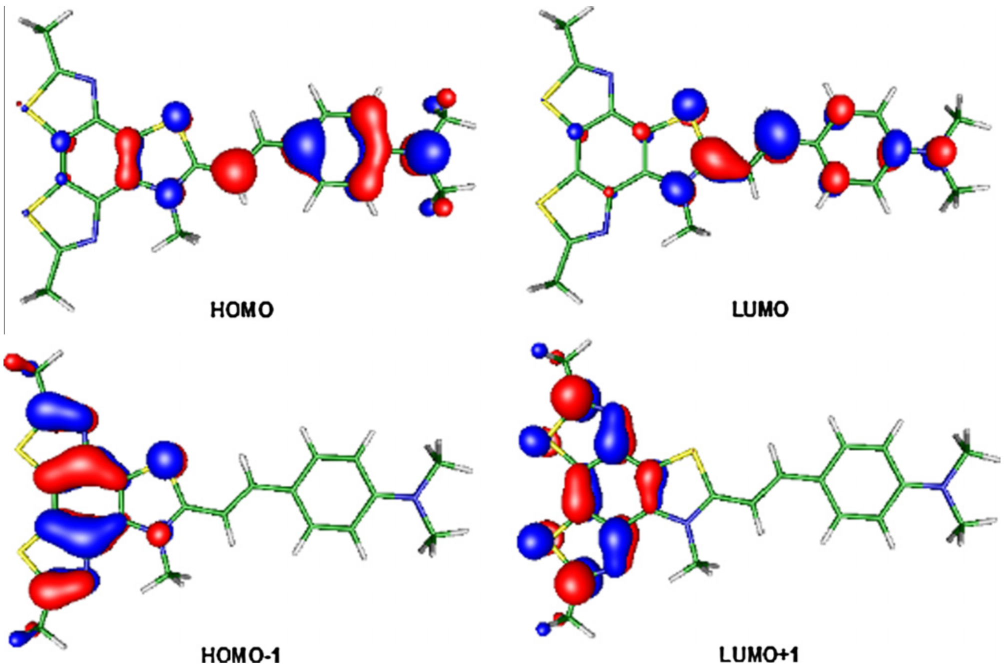

Fig. 8. Relevant molecular orbitals (isosurface ±0.04 au) in the compound **3a**.

in higher Φ_F values for chromophores with longer conjugated bridge. The Stokes shift is also enlarged with the prolongation of conjugation. The smallest Stokes shift was observed in compound **3f** with julolidine donor and could be explained by the more similar values of the excited and ground state dipole moments. While in compounds **3a**–**3e** the dipole moment of the excited state differs more from the ground state's one, in compound **3f**, owing to better conjugation, the important charge transfer have already occurred in the ground state. The modest difference in the charge transfer character of excited and ground state is the reason of small Stokes shift in **3f**.

Fig. 8 presents an orbital picture of cation 3a. Highest occupied molecular orbital (HOMO) is predominantly located on the donor part (dimethylamino and phenyl) whereas in the lowest unoccupied molecular orbital (LUMO) the orbital density is moved to the thiazolium part of the heterocyclic core and conjugated bridge. This corresponds with the lowest energy excitation (ICT band) which is represented almost exclusively (more than 97%) by the HOMO–LUMO transition. Orbitals HOMO − 1 as well as LUMO + 1 are localized in the benzotristhiazolium part of the cation.

4. Conclusion

The unsymmetrical electron-withdrawing benzotristhiazole core prepared via six-step synthesis was further treated with the aim to design chromophores with possible application in nonlinear optics. Methylation of the central unit led to a monomethylated benzotristhiazolium salt which structure was solved by X-ray analysis and corroborated by quantum-chemical DFT-B3LYP study. Six novel push–pull salts have been synthetized by the Knoevenagel type condensation and studied by spectral (UV–Vis, fluorescence) and theoretical methods.

The increasing number of double bonds in conjugated bridge as well as diphenylamino substituent as a strong donor group enhance the nonlinear optical response represented by the calculated hyperpolarizabilities β and γ. Finally, the structure of a new chromophore tailored by the combination of the best fragments was predicted and a high value of β was obtained by theoretical calculations that agree with the prediction.

Supplementary material

The deposition number CCDC 876258 for compound **2b** contains the supplementary crystallographic data for this paper. These data can be obtained free of charge via www.ccdc.cam.ac.uk/data_request/cif or Cambridge Crystallographic Data Center, 12 Union Road, Cambridge CB2 1EZ, UK; fax: +44 1223 336033.

Acknowledgements

This work has been supported by the Slovak Grant Agency APVV (Grants APVV 0259-07, APVV 0424-10 and APVV 0262-10) and also by the Slovak Grant Agency for Science (Grant no. 1/1126/11). The financial support is gratefully acknowledged. A.F. thanks for the Comenius University Grants (No. UK/56/2010, UK/259/2009). We also thank the Structural Funds, Interreg IIIA for the financial support in purchasing the diffractometer.

References

[1] E. de Meulenaere, W.-Q. Chen, S. van Cleuvenbergen, M.-L. Zheng, S. Psilodimitrakoupoulos, R. Paesen, J.-M. Taymans, M. Ameloot, J. Vanderleyden, P. Loza-Alvarez, X.-M. Duan, K. Clays, Chem. Sci. 3 (2012) 984.
[2] M.-L. Zheng, K. Fujita, W.-Q. Chen, N.I. Smith, X.-M. Duan, S. Kawata, ChemBioChem 12 (2011) 52.
[3] C. Huang, M.M. Sartin, N. Siegel, M. Cozzuol, Y. Zhang, J.M. Hales, S. Barlow, J.W. Perry, S.R. Marder, J. Mater. Chem. 21 (2011) 16119.
[4] L. Beverina, M. Crippa, M. Landenna, R. Ruffo, P. Salice, F. Silvestri, S. Versari, A. Villa, L. Ciaffoni, E. Collini, C. Ferrante, S. Bradamente, C.M. Mari, R. Bozio, G. Pagani, J. Am. Chem. Soc. 130 (2008) 1894.
[5] F. Hao, X. Zhang, Y. Tian, H. Zhou, L. Li, J. Wu, S. Zhang, J. Yang, B. Jin, X. Tao, G. Zhou, M. Jiang, J. Mater. Chem. 19 (2009) 9163.
[6] J. Lott, C. Ryan, B. Valle, J.R. Johnson III, D.A. Schiraldi, J. Shan, K.D. Singer, C. Weder, Adv. Mater. 23 (2011) 2425.
[7] S. Maruo, J.T. Fourkas, Laser Photonics Rev. 2 (2008) 100.
[8] A. Abbotto, L. Beverina, R. Bozio, A. Facchetti, C. Ferrante, G.A. Pagani, D. Pedron, R. Signorini, Org. Lett. 4 (2002) 1495.
[9] M.M.M. Raposo, A.M.C. Fonseca, M.C.R. Castro, M. Belsley, M.F.S. Cardoso, L.M. Carvalho, P.J. Coelho, Dyes Pigments 91 (2011) 62.

[10] M.M.M. Raposo, M.C.R. Castro, M. Belsley, A.M.C. Fonseca, Dyes Pigments 91 (2011) 454.
[11] P.J. Coelho, M.C.R. Castro, A.M.C. Fonseca, M.M.M. Raposo, Dyes Pigments 92 (2012) 745.
[12] D. Beljonne, W. Wenseleers, E. Zojer, Z. Shuai, H. Vogel, S.J.K. Pond, J.W. Perry, S.R. Marder, J.-L. Brédas, Adv. Funct. Mater. 12 (2002) 631.
[13] A. Abotto, L. Beverina, S. Bradamante, A. Facchetti, G.A. Pagani, R. Bozio, C. Ferrante, D. Pedron, R. Signorini, Synth. Metals 139 (2003) 795.
[14] A. Fülöpová, P. Magdolen, M. Károlyiová, I. Sigmundová, P. Zahradník, J. Het. Chem. (2012), http://dx.doi.org/10.1002/jhet.1530.
[15] T. Karstens, K. Kobs, J. Phys. Chem. 84 (1980) 1871.
[16] D. Plazuk, I. Janowska, A. Klys, A. Hameed, J. Zakrzewski, Synth. Commun. 33 (2003) 381.
[17] J.M. Kauffman, G. Moyna, J. Org. Chem. 68 (2003) 839.
[18] P. Hrobárik, I. Sigmundová, P. Zahradník, P. Kasák, V. Arion, E. Franz, K. Clays, J. Phys. Chem. C 114 (2010) 22289.
[19] H. Wang, Z. Lu, S.J. Lord, K.A. Willets, J.A. Bertke, S.D. Bunge, W.E. Moerner, R.J. Twieg, Tetrahedron 63 (2007) 103.
[20] Agilent Technologies, CrysAlisPro 1.171.35.21, Agilent Technologies UK Ltd., Oxford, UK, 2012.
[21] M.C. Burla, R. Caliandro, M. Camalli, B. Carrozzini, G.L. Cascarano, C. Giacovazzo, M. Mallamo, A. Mazzone, G. Polidori, R. Spagna, J. Appl. Cryst. 45 (2012) 357.
[22] G.M. Sheldrick, Acta Cryst. Sect. A 64 (2008) 112.
[23] K. Brandenburg, DIAMOND 3.2g, Crystal Impact GbR, Bonn, Germany, 2011.
[24] C.F. Macrae, I.J. Bruno, J.A. Chisholm, P.R. Edgington, P. McCabe, E. Pidcock, L. Rodriguez-Monge, R. Taylor, J. van de Streek, P.A. Wood, J. Appl. Cryst. 41 (2008) 466.
[25] TURBOMOLE V6.2 2010, a development of University of Karlsruhe and Forschungszentrum Karlsruhe GmbH, 1989–2007, TURBOMOLE GmbH, since 2007.
[26] O. Treutler, R. Ahlrichs, J. Chem. Phys. 102 (1995) 346.
[27] (a) A.D. Becke, J. Chem. Phys. 98 (1993) 5648;
(b) C. Lee, W. Yang, R.G. Parr, Phys. Rev. B 37 (1988) 785.
[28] A. Schäfer, C. Huber, R. Ahlrichs, J. Chem. Phys. 100 (1994) 5829.
[29] U.C. Singh, P.A. Kollman, J. Comput. Chem. 5 (1984) 129.
[30] F. Furche, D. Rappoport, Density functional theory for excited states: equilibrium structure and electronic spectra, in: M. Olivucci (Ed.), Computational and Theoretical Chemistry, vol. 16, Elsevier, Amsterdam, 2005 (Chapter III of Computational Photochemistry).
[31] H.A. Kurtz, J.J.P. Stewart, K.M. Dieter, J. Comput. Chem. 11 (1990) 82.
[32] (a) J.J.P. Stewart, J. Comput. Chem. 10 (1989) 209;
(b) J.J.P. Stewart, J. Comput. Chem. 10 (1989) 221;
(c) J.J.P. Stewart, J. Comput. Chem. 12 (1991) 320.
[33] Ampac 8, 1992–2004 Semichem, Inc. PO Box 1649, Shawnee, KS 66222.
[34] (a) G.A. Jeffrey, L. Lewis, Carbohydr. Res. 60 (1978) 179;
(b) R. Taylor, O. Kennard, Acta Cryst. B 39 (1983) 133.
[35] I. Sigmundová, P. Zahradník, D. Loos, Collect. Czech. Chem. Commun. 72 (2007) 1069.
[36] Y. Hong, J.W.Y. Lam, B.Z. Tang, Chem. Soc. Rev. 40 (2011) 5361.